DOI: 10.31114/2078-7707-2022-4-228-233

TCAD Simulation of Sacrificial Layer Etching in Sensitive Element of IR Microbolometer Array Based on SOI Structure

I.D. Evsikov[1], G.D. Demin[1], N.A. Djuzhev[1], E.A. Fetisov[1,2], R.Z. Khafizov[2,3]

[1]National Research University of Electronic Technology (MIET), Moscow, Zelenograd, Russia, gddemin@edu.miet.ru

[2]Liv MOS Engineering LLC, Moscow, Zelenograd, Russia

[3]GraphImpress Co., Ltd., Moscow, Russia

***Abstract* — Currently, the development of uncooled IR microbolometer arrays based on SOI structures attracts significant attention of researchers, due to their high speed and temperature sensitivity compared to other bolometric and thermocouple sensor elements operating in the IR wavelength spectrum. An important parameter of such SOI-based IR microbolometers is the useful area of the dielectric (SiO_2) membrane that absorbs IR radiation and its high thermal insulation, which requires technological optimization of the sacrificial layer (Si) etching modes through a matrix of holes (windows) in the SiO_2 membrane. In this work, TCAD simulation of the gas-phase etching of the sacrificial Si layer was carried out, taking into account both its thickness and the size of the windows. It was shown that a decrease in the window size from 120 to 80 μm^2 leads to a twofold decrease in the etching time (from 480 to 240 seconds) and provides an effective increase in the useful surface of the microbolometer sensing element, which is heated by IR radiation. The obtained results can be useful in the process of working out technological operations for the fabrication of IR microbolometer arrays based on SOI substrates.**

***Keywords* — MEMS technology, uncooled IR microbolometer, SOI structure, chemical etching, TCAD simulation, thermocouples, thermal sensor, sacrificial layer, dielectric membrane.**

I. INTRODUCTION

The potential capabilities of modern silicon technology make it possible to use a class of uncooled thermal sensors for detecting infrared (IR) radiation, the operation of which is based on various physical effects. In particular, among them are thermoresistive IR bolometers [1], IR bolometers based on the thermoelectric Seebeck effect [2], pyro- and ferroelectric IR sensors [3, 4], IR sensors based on chalcogenide glasses [5], IR sensors based on quantum dots [6]. The world's leading electronic companies (Honeywell (USA), Raytheon (USA), BAE Systems (Great Britain), Lynred (France), Leonardo DRS (USA)) are making serious efforts to set up and conduct research and development in order to determine the most effective ways to implement such IR thermal sensors. The results obtained in this direction have made it possible to create multi-element IR receivers with thermal sensors based on the Micro-Electro-Mechanical Systems (MEMS) technology, the operation of which is based on the use of thermoresistive and thermoelectric effects [7]. By their physical nature, these effects are independent of the composition of IR spectrum. Accordingly, in contrast to quantum IR receivers, the sensitivity of thermal IR sensors generally does not depend on the wavelength. At the same time, the spectral range of sensitivity of the thermal IR sensors can be adjusted by selecting corresponding materials that are responsible for efficient heat absorption in the sensitive elements. Serious interest in thermal sensors arose when thermal IR image detectors began to overcome the sensitivity barrier corresponding to the value of the noise equivalent temperature difference (NETD) at the level of about 100 mK [8, 9]. The first commercial thermal photodetectors with bolometric arrays with a degree of integration of 320x240 pixels and a pixel size of about 50 μm already had a NETD significantly lower than 100 mK [10, 11].

The manufacturing technology for all types of thermal sensors that can be integrated into multi-element IR receivers is based on the MEMS technology for the fabrication of nano-sized dielectric membranes with highly efficient heat-absorbing coatings from materials such as black absorbing materials (Au, Pt, Si, C) [12-14], SiN_X [15], or from metamaterial perfect absorbers in the IR region based on metal-dielectric-metal periodic nanostructures [16]. The membrane in such thermal IR sensors is suspended above a silicon substrate on consoles that poorly conduct heat, and therefore it has good thermal insulation. Having a low thermal mass, the membrane structure is able to quickly heat up under the action of IR radiation. A main advantage of the MEMS fabrication process is that it can be easily integrated into standard CMOS technology. The most impressive progress in the development of thermal array detectors has been achieved using thermoresistive MEMS-based sensitive elements (microbolometers) as thermal sensors [17]. The development of the design and technology of microbolometric array detectors in recent years has mainly been directed to the implementation of pixels with small (down to 12 μm [18]) sizes while maintaining their high sensitivity. Advances in miniaturization have made it

possible to create ultra-large IR arrays with high resolution thermal imaging [19]. Modern technology for creating microbolometric thermal sensors demonstrates the possibility of creating IR arrays with the number of elements up to 2048 x 1536 [20].

Since the use of high-tech single-crystal silicon with its high Seebeck coefficient (up to the level of 1 mV/K and higher [21]) is attractive as a material for thermocouple elements, the silicon-on-insulator (SOI) structure seems very promising as the functional material for uncooled IR microbolometer arrays [22, 23]. In this regard, one of the important technological problems in the design of microbolometric arrays based on SOI structures is to provide good thermal insulation of the sensitive membrane layer while maintaining a large usable area that absorbs IR radiation. In turn, this requires the selection of optimal modes of local etching of the sacrificial silicon (Si) layer under the membrane to form a cavity in the SOI structure. For this purpose, as a rule, holes are formed in the membrane, the shape, size and number of which will affect the final relief of the cavity bottom and the corresponding rate/time of etching of the sacrificial layer. In this work, the technology computer-aided design (TCAD) tool is used to simulate the etching process of the sacrificial layer in the proposed structure of the sensitive element of an IR microbolometer sensor operating on the thermoelectric effect in a matrix of series-connected thermocouples on a suspended membrane with a set of holes (Fig. 1).

Such a theoretical analysis of the technological process of etching the SOI structure of a microbolometer through a perforated membrane meets the current needs of developers of modern heat-detection equipment to increase the performance of IR optoelectronic systems based on thermal detector arrays.

II. Design of the IR Microbolometer Element

The proposed design of the matrix element of an IR microbolometer sensor with lateral dimensions of 112 x 112 μm^2 is schematically shown in Fig. 1. The sacrificial layer is a hidden layer of silicon (Si) in the SOI structure (shown in blue), while the thermosensitive element belongs to the single-crystal Si layer of SOI substrate (shown in green) and determines the IR heating temperature of the dielectric (SiO_2) membrane (shown in gray) with the top SiN_X layer (shown in purple). Readout circuits can be formed in a single-crystal Si layer, for which it is initially used in an SOI structure.

The SOI structure is used as a substrate in a matrix element due to the fact that single-crystal Si is one of the widely used and technologically promising materials for micro- and nanoelectronics.

The cross section of the corresponding element of the microbolometer matrix with a set of thermocouples is shown in Fig. 2. As shown in the figure, a thin-film SiO_2 membrane suspended on elastic consoles has a set of holes designed to etch the sacrificial Si layer in the SOI substrate in order to form a cavity for thermal insulation of the membrane. The SiN_X layer that covers the central part of the membrane is used to increase the efficiency of the absorption of IR radiation. According to Fig. 2, n+/p+ poly-Si (Si*) thermocouples are located on the periphery of the membrane to read the heating temperature of the membrane structure of the matrix microbolometer element and then convert it into an electrical signal (thermo-voltage).

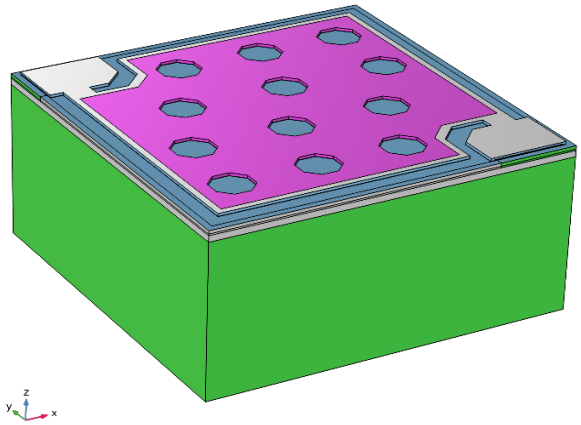

(a)

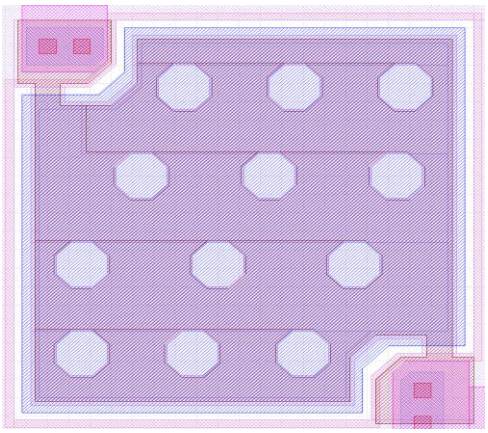

(b)

Fig. 1. The design of the sensitive element of the microbolometer IR sensor based on the SOI structure: (a) the model of the element in a CAD-oriented software package (COMSOL MultiPhysics), (b) the topology of the element

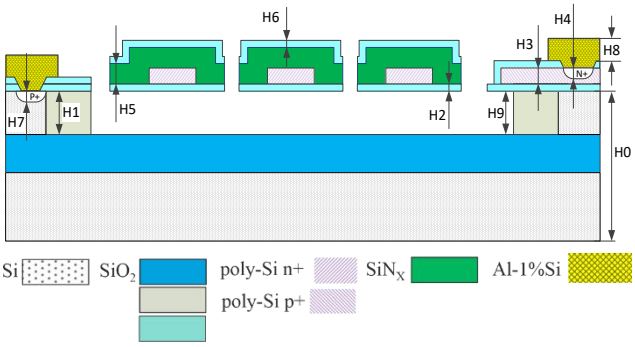

Fig. 2. The cross section of the sensitive element of microbolometer IR array based on the SOI structure with a sacrificial Si layer and a set of n+/p+ Si* thermocouples

Table 1 summarizes the parameters of the layers of the selected design of the microbolometer matrix element, which were taken in accordance with the with the developed process flow for fabrication of the experimental samples of the sensor. The thickness of the sacrificial Si layer and the depth of the cavity formed under the membrane were taken by default to be 1 μm.

Table 1

Parameters of the layers of the microbolometer IR matrix element with series-connected thermocouples

Structure elements		Thickness, μm	Resistivity	Material
Name of the layer	Symbol			
SOI substrate Ø150 mm	H0	1.0/2.0/675	12 Ω·cm	$Si/SiO_2/Si$ Si doped with boron (B) –(100)
Insulating groove	H1	1.0	-	SiO_2
Dielectric	H2	0.10±0.01	-	SiO_2
N-type poly-Si (Si*) (thermistor)	H3	0.25±0.05	100 kΩ/sq.	Si*
N+-type poly-Si*	H4	0.25±0.05	80 Ω/sq.	Si*
Temperature sensitive membrane	H5	0.60±0.05	-	SiNx
Protective dielectric	H6	0.15±0.01	-	SiO_2
P+ sub-doping	H7	0.25±0.05	100 Ω/sq.	Si
Metallization	H8	1.0±0.1	0.04 Ω/sq.	Al-1%Si
Sacrificial Si layer (SOI device layer)	H9	1.0±0.01	12 Ω·cm	Si

III. DESCRIPTION OF THE PROCESS OF TCAD SIMULATION

To perform the simulation of the process of gas-phase (plasma-chemical) etching of the sacrificial Si layer of SOI substrate in XeF_2, commercial Silvaco TCAD software package was used [24]. The initial stage before the simulation was to select a fragment (pattern) of the topology of microbolometer sensitive element, which is shown in Fig. 3.

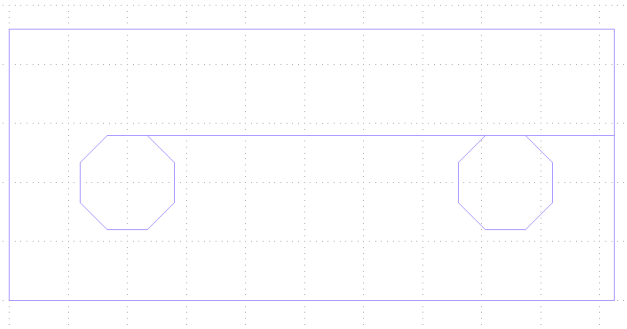

Fig. 3. A pattern of the topology of the sensitive element of the microbolometric IR array with two windows (holes in SiO2 membrane for etching the sacrificial Si layer)

The selected pattern of the topology has two windows – holes in the form of an octagon in the SiO_2 membrane layer of the sensing element for etching the sacrificial Si layer located under the membrane. To select the optimal sizes of windows (holes) in the membrane layer for etching the sacrificial layer, their area was varied. To illustrate the etching process, the following window areas were taken: 40 μm^2; 80 μm^2; 120 μm^2. As a result, three patterns of the topology of the sensing element were formed. The topology patterns were imported into the lithographic mask design module (Maskviews) included in the Silvaco TCAD software package (Fig. 4).

Based on the imported files, masks for simulating the Si gas-phase etching process were created, which exactly repeated the patterns of the selected fragments.

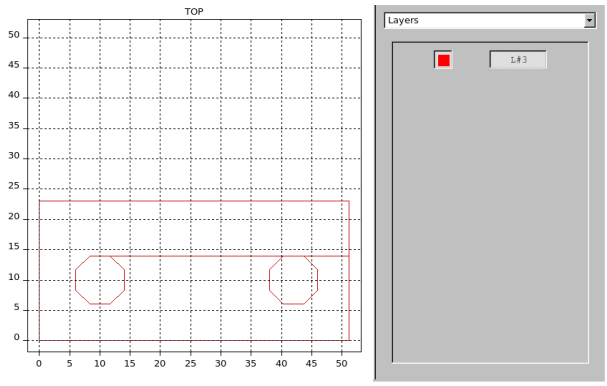

Fig. 4. Image of a lithographic mask built on the basis of a topology pattern with two windows (holes) and loaded into the Maskviews module

The simulation of the process of gas-phase etching of the sacrificial Si layer in the XeF_2 atmosphere was carried out in the Victory Process module of the Silvaco TCAD software environment. The cross-sectional model of the structure of the sensitive element of the microbolometer was formed from four alternating layers of Si and SiO_2 using the operation of ideally conformal layer deposition. The thickness of each of the layers of the structure was set according to Table 1, except for the bottom Si layer, the thickness of which was chosen to be 1 μm to simplify the simulation, since this layer does not affect the etching process of the top sacrificial Si layer. The width of the structure was limited by the width of the imported patterns of the device topology (~52 μm). The structure obtained in the Victory Process module after opening windows in the SiO_2 membrane layer for the purpose of subsequent etching of the sacrificial Si layer is shown in Fig. 5. To carry out the process of gas-phase etching of the sacrificial Si layer, an ideal isotropic etching model was chosen. The rate of isotropic etching of Si was set on the basis of the technical documentation for the operation of the Xactix gas-phase etching module [25]: 2 μm/min for etching Si through narrow slots in the masking layers.

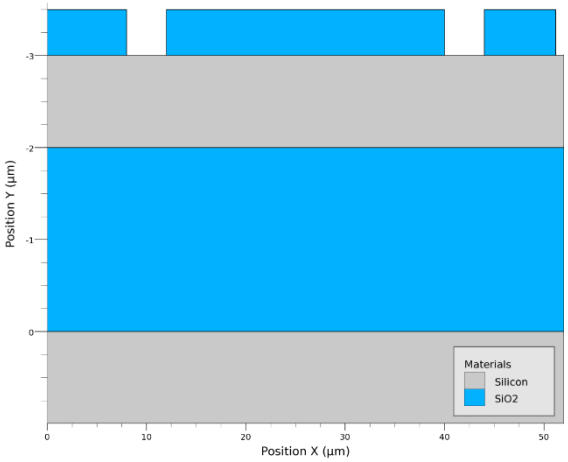

Fig. 5. Layer-by-layer structure of the sensitive element of the microbolometric IR array after the stage of opening windows in the SiO_2 layer, obtained in the Victory Process module of the Silvaco TCAD software environment

Due to the rather large width of the model (52 μm) and, as a result, the insufficiently high resolution of the computational grid to reproduce fine details of the etching relief, as well as the high selectivity of SiO_2 to Si etching (1000:1), the SiO_2 etching rate was taken equal to 0.

IV. Results

The corresponding profiles of the structure formed after etching the sacrificial Si layer for the selected three fragments of the topology of the microbolometer matrix element with different window areas in the SiO_2 layer of the membrane (40 μm^2; 80 μm^2; 120 μm^2) are shown in Fig. 6-8. To illustrate the process of formation of the relief of each structure, different values of the time of the etching process were set.

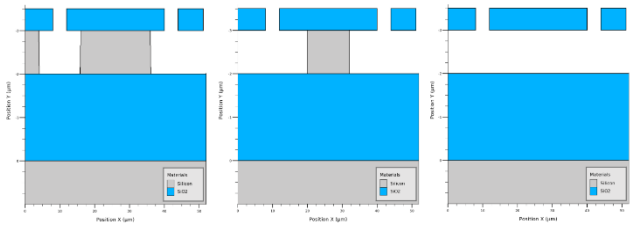

Fig. 6. Etching profiles of the sacrificial silicon (Si) layer of the sensitive element of the IR microbolometric array for two windows with an area of 40 μm^2. Specified etching time: (a) 120 s; (b) 240 s; (c) 480 s

Based on the data obtained, the dependence of the gas-phase etching time of the sacrificial Si layer on the window area was calculated (Fig. 9).

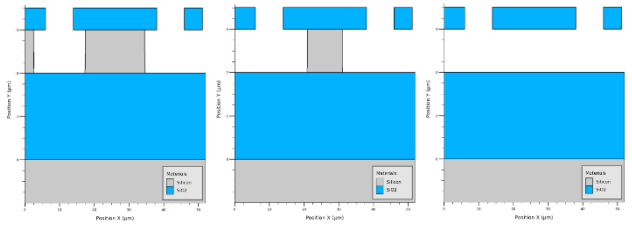

Fig. 7. Etching profiles of the sacrificial silicon (Si) layer of the sensitive element of the IR microbolometric array for two windows with an area of 80 μm^2. Specified etching time: (a) 105 s; (b) 210 s; (c) 420 s

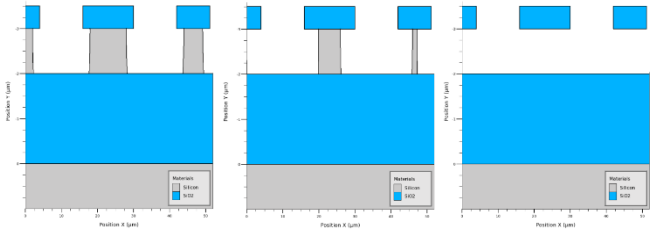

Fig. 8. Etching profiles of the sacrificial silicon (Si) layer of the sensitive element of the IR microbolometric array for two windows with an area of 120 μm^2. Specified etching time: (a) 60 s; (b) 120 s; (c) 240 s

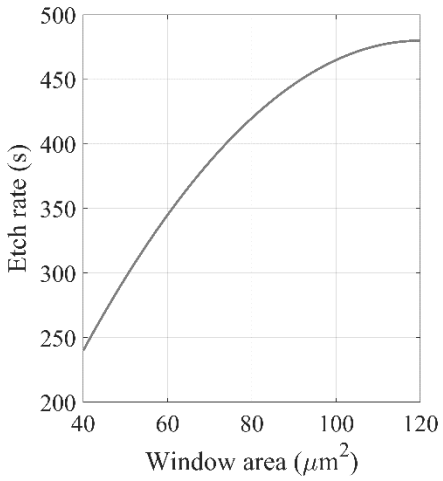

Fig. 9. Calculated time of gas-phase etching of the sacrificial Si layer in XeF2 as a function of the area of the windows in the SiO_2 membrane layer of a single element of the IR microbolometer array

According to Fig. 9, the etching time of the sacrificial layer with a thickness of 1 μm increases non-linearly with the increase in the area of windows (holes in SiO2 layer (membrane) of SOI substrate), while the choice of a smaller diameter of the windows makes it possible to achieve efficient etching and provide a large useful surface area of the microbolometer that absorbs IR radiation.

V. Conclusions

The TCAD simulation of the etching of the sacrificial Si layer through windows (holes) in the sensitive SiO2 membrane of the microbolometer array was carried out. It was shown that a decrease in the window size from 120 to 40 μm2 leads to a decrease in the layer removal time by almost a factor of 2 (from 480 to 240 s) at a given etching rate (2 μm/min), which can be used to achieve a larger usable membrane area for effective absorption of incident IR radiation.

Acknowledgement

The work was performed at Liv MOS Engineering Ltd. company based on the equipment of MIET Core Facilities Center «MEMSEC» (MIET) and supported by the Ministry of Education and Science of Russian Federation (Agreement № 075-15-2021-1350, 05.10.2021 (internal number 15.SIN.21.0004)).

References

[1] Yadav P.V.K. et al. Advancements of uncooled infrared microbolometer materials: A review // Sensors and Actuators A: Physical. 2022. V. 342. P. 113611.

[2] Xu D. et al. MEMS-based thermoelectric infrared sensors: A review // Front. Mech. Eng. 2017. V. 12. № 4. P. 557–566.

[3] Li H., Bowen C.R., Yang Y. Phase transition enhanced pyroelectric nanogenerators for self-powered temperature sensors // Nano Energy. 2022. V. 102. P. 107657.

[4] Ranu et al. CMOS compatible pyroelectric materials for infrared detectors // Materials Science in Semiconductor Processing. 2022. V. 140. P. 106375.

[5] Kang S. et al. Chalcogenide glass for thermoelectric application // Journal of Non-Crystalline Solids: X. 2022. V. 15. P. 100111.

[6] Hafiz S.B. et al. Colloidal quantum dots for thermal infrared sensing and imaging // Nano Convergence. 2019. V. 6, № 1. P. 7.

[7] Mbarek S.B., Alcheikh N., Younis M.I. Recent advances on MEMS based Infrared Thermopile detectors // Microsyst Technol. 2022. V. 28, № 8. P. 1751–1764.

[8] Chatard J.-P., Tribolet P.M. Uncooled infrared detector technology from research to production within six months / ed. Brown G.J., Razeghi M. San Jose, CA, 2001. P. 100–111.

[9] Norton P.W. et al. Commercialization of uncooled infrared technology / ed. Dereniak E.L., Sampson R.E., Johnson C.B. Denver, CO, 2004. P. 55.

[10] Niklaus F., Vieider C., Jakobsen H. MEMS-based uncooled infrared bolometer arrays: a review / ed. Chiao J.-C. et al. Beijing, China, 2007. P. 68360D.

[11] Belin A.M., Zolotarev V.I., Nikiforov A. Yu., Popov A.D. KMOP-matrica formata 320x240 elementov dlya spektral'nogo diapazona 3-5 mkm na osnove PtSi // Izvestiya vyzov. Electronica (Proceedings of universities. Electronics), 2015. № 3. P. 246–251.

[12] Steglich M. et al. An ultra-black silicon absorber: An ultra-black silicon absorber // Laser & Photonics Reviews. 2014. V. 8, № 2. P. L13–L17.

[13] Smith E.M. et al. Dual band sensitivity enhancements of a VO_x microbolometer array using a patterned gold black absorber // Appl. Opt. 2016. V. 55, № 8. P. 2071.

[14] Suen J.Y. et al. Multifunctional metamaterial pyroelectric infrared detectors // Optica. 2017. Vol. 4, № 2. P. 276.

[15] Stocchi M. et al. Mid-infrared optical characterization of thin SiN x membranes // Appl. Opt. 2019. V. 58, № 19. P. 5233.

[16] Zhou Y. et al. Ultra-broadband metamaterial absorbers from long to very long infrared regime // Light Sci Appl. 2021. V. 10, № 1. P. 138.

[17] Demin G.D. et al. Modeling the Electromechanical Properties of the MEMS Element of a Thermoelectric Infrared Sensor Based on the Dynamic Seebeck Effect // 2020 21st International Conference of Young Specialists on Micro/Nanotechnologies and Electron Devices (EDM). Chemal, Russia: IEEE, 2020. P. 298–303.

[18] Becker S. et al. Latest pixel size reduction of uncooled IR-FPA at CEA, LETI / ed. Huckridge D.A., Ebert R.R. Edinburgh, United Kingdom, 2012. P. 85410C.

[19] Zhou W. et al. Single-side micromachined ultra-small thermopile IR detecting pixels for dense-array integration // J. Micromech. Microeng. 2022. V. 32, № 5. P. 055003.

[20] S.M. Johnson and E.P.G. Smith, Next Generation EO/IR Detectors // Raytheon Technology Today. 2014. № 1. P. 22-23.

[21] Salleh F. et al. Seebeck Coefficient of Ultrathin Silicon-on-Insulator Layers // Appl. Phys. Express. 2009. V. 2. P. 071203.

[22] Yu L. et al. Low-Cost Microbolometer Type Infrared Detectors // Micromachines. 2020. V. 11, № 9. P. 800.

[23] Froberger K. et al. SOI-based micro-mechanical terahertz detector operating at room-temperature and atmospheric pressure // Appl. Phys. Lett. 2022. V. 120, № 26. P. 261103.

[24] URL: https://silvaco.com/tcad (access date: 30.08.2022)

[25] URL: https://wiki.nanotech.ucsb.edu/w/images/7/7b/Xactic-XetchX3-System-Manual.pdf (access date: 30.08.2022)

Приборно-технологическое моделирование травления жертвенного слоя в чувствительном элементе микроболометрической ИК матрицы на базе КНИ структуры

И.Д. Евсиков[1], Г.Д. Демин[1], Н.А. Дюжев[1], Е.А. Фетисов[1,2], Р.З. Хафизов[2,3]

[1]Национальный исследовательский университет «Московский институт электронной техники» (МИЭТ), Москва, Зеленоград, Россия, gddemin@edu.miet.ru

[2]ООО «Лив МОС Инжиниринг», Москва, Зеленоград, Россия

[3]ООО «ГрафИмпресс», Москва, Россия

***Аннотация* — В настоящее время большое внимание исследователей привлекает разработка неохлаждаемых ИК матричных микроболометров на базе КНИ структур, что обусловлено их высоким быстродействием и температурной чувствительностью по сравнению с другими болометрическими и термопарными сенсорными элементами, работающими в ИК спектре длин волн. Важным параметром таких КНИ микроболометров является полезная площадь диэлектрической (SiO_2) мембраны, поглощающей ИК излучение, и ее хорошая тепловая изоляция, что требует технологического подбора режимов травления жертвенного слоя (Si) через матрицу сквозных отверстий (окон) в SiO_2 мембране. В работе проведено TCAD моделирование газофазного травления жертвенного Si слоя с учётом его толщины и размера окон. Показано, что уменьшение размера окон от 120 до 80 мкм^2 приводит к снижению в 2 раза времени травления (от 480 до 240 секунд) и обеспечивает эффективное увеличение полезной поверхности чувствительного элемента микроболометра, которая разогревается от ИК излучения. Полученные результаты могут быть полезны в процессе отработки технологических операций изготовления ИК микроболометрических матриц на КНИ подложках.**

***Ключевые слова* — МЭМС технология, неохлаждаемый ИК микроболометр, КНИ структура, химическое травление, TCAD моделирование, термопары, тепловой сенсор, жертвенный слой, диэлектрическая мембрана.**

REFERENCES

[1] Yadav P.V.K. et al. Advancements of uncooled infrared microbolometer materials: A review // Sensors and Actuators A: Physical. 2022. V. 342. P. 113611.

[2] Xu D. et al. MEMS-based thermoelectric infrared sensors: A review // Front. Mech. Eng. 2017. V. 12. № 4. P. 557–566.

[3] Li H., Bowen C.R., Yang Y. Phase transition enhanced pyroelectric nanogenerators for self-powered temperature sensors // Nano Energy. 2022. V. 102. P. 107657.

[4] Ranu et al. CMOS compatible pyroelectric materials for infrared detectors // Materials Science in Semiconductor Processing. 2022. V. 140. P. 106375.

[5] Kang S. et al. Chalcogenide glass for thermoelectric application // Journal of Non-Crystalline Solids: X. 2022. V. 15. P. 100111.

[6] Hafiz S.B. et al. Colloidal quantum dots for thermal infrared sensing and imaging // Nano Convergence. 2019. V. 6, № 1. P. 7.

[7] Mbarek S.B., Alcheikh N., Younis M.I. Recent advances on MEMS based Infrared Thermopile detectors // Microsyst Technol. 2022. V. 28, № 8. P. 1751–1764.

[8] Chatard J.-P., Tribolet P.M. Uncooled infrared detector technology from research to production within six months / ed. Brown G.J., Razeghi M. San Jose, CA, 2001. P. 100–111.

[9] Norton P.W. et al. Commercialization of uncooled infrared technology / ed. Dereniak E.L., Sampson R.E., Johnson C.B. Denver, CO, 2004. P. 55.

[10] Niklaus F., Vieider C., Jakobsen H. MEMS-based uncooled infrared bolometer arrays: a review / ed. Chiao J.-C. et al. Beijing, China, 2007. P. 68360D.

[11] Белин А.М., Золотарев В.И., Никифоров А. Ю., Попов А.Д. КМОП-матрица формата 320x240 элементов для спектрального диапазона 3-5 мкм на основе PtSi // Известия вузов. Электроника, 2015. № 3. С. 246–251.

[12] Steglich M. et al. An ultra-black silicon absorber: An ultra-black silicon absorber // Laser & Photonics Reviews. 2014. V. 8, № 2. P. L13–L17.

[13] Smith E.M. et al. Dual band sensitivity enhancements of a VO_x microbolometer array using a patterned gold black absorber // Appl. Opt. 2016. V. 55, № 8. P. 2071.

[14] Suen J.Y. et al. Multifunctional metamaterial pyroelectric infrared detectors // Optica. 2017. Vol. 4, № 2. P. 276.

[15] Stocchi M. et al. Mid-infrared optical characterization of thin SiN x membranes // Appl. Opt. 2019. V. 58, № 19. P. 5233.

[16] Zhou Y. et al. Ultra-broadband metamaterial absorbers from long to very long infrared regime // Light Sci Appl. 2021. V. 10, № 1. P. 138.

[17] Demin G.D. et al. Modeling the Electromechanical Properties of the MEMS Element of a Thermoelectric Infrared Sensor Based on the Dynamic Seebeck Effect // 2020 21st International Conference of Young Specialists on Micro/Nanotechnologies and Electron Devices (EDM). Chemal, Russia: IEEE, 2020. P. 298–303.

[18] Becker S. et al. Latest pixel size reduction of uncooled IR-FPA at CEA, LETI / ed. Huckridge D.A., Ebert R.R. Edinburgh, United Kingdom, 2012. P. 85410C.

[19] Zhou W. et al. Single-side micromachined ultra-small thermopile IR detecting pixels for dense-array integration // J. Micromech. Microeng. 2022. V. 32, № 5. P. 055003.

[20] S.M. Johnson and E.P.G. Smith, Next Generation EO/IR Detectors // Raytheon Technology Today. 2014. № 1. P. 22-23.

[21] Salleh F. et al. Seebeck Coefficient of Ultrathin Silicon-on-Insulator Layers // Appl. Phys. Express. 2009. V. 2. P. 071203.

[22] Yu L. et al. Low-Cost Microbolometer Type Infrared Detectors // Micromachines. 2020. V. 11, № 9. P. 800.

[23] Froberger K. et al. SOI-based micro-mechanical terahertz detector operating at room-temperature and atmospheric pressure // Appl. Phys. Lett. 2022. V. 120, № 26. P. 261103.

[24] URL: https://silvaco.com/tcad (access date: 30.08.2022).

[25] URL: https://wiki.nanotech.ucsb.edu/w/images/7/7b/Xactic-XetchX3-System-Manual.pdf (access date: 30.08.2022).